# Lithium Intercalation in Anatase−Structural and Magnetic Considerations

Vittorio Luca,*,† Brett Hunter,‡ Boujemaa Moubaraki,§ and Keith S. Murray§

*School of Chemistry, University of New South Wales, Sydney, NSW 2053, Australia, and Physics Division, Australian Nuclear Science and Technology Organization, PMB 1, Menai, NSW 2234, Australia, and Department of Chemistry, Monash University, Clayton, Victoria 3168, Australia*

*Received June 20, 2000. Revised Manuscript Received December 5, 2000*

The intercalation of Li in anatase to give orthorhombic $Li_xTiO_2$ compounds with $x$ in the range 0−0.7 has been studied. Neutron diffraction patterns have been measured and refined as a function of $x$ to shed light on the mechanism of the intercalation reaction. It appears that transformation of tetragonal anatase to the orthorhombic structure is preceded by an initial expansion of the anatase unit cell. As $x$ increases, most of the added electrons fill the anatase conduction band and susceptibility measurements indicate that an insulator-to-metal transition occurs for $x > 0.3$. Electron paramagnetic resonance and susceptibility measurements indicate that only very few of the injected electrons are localized on Ti to give $Ti^{3+}$.

## Introduction

The reversible topotactic redox intercalation of lithium in oxide hosts is an important process in rechargeable lithium ion (rocking-chair) batteries and electrochromic devices[1] and a possible soft chemical (*chimie douce*) route to novel oxide materials. The advantages of this light oxide in battery applications are that (1) the energy density is potentially very high, (2) the Ti cations appear to be difficult to reduce to the metal, suggesting good long-term stability,[2] and (3) titania is an environmentally benign oxide.

The intercalation of Li in anatase using *n*-butyllithium occurs stoichiometrically up to a composition of $Li_{0.5}TiO_2$. Cava et al.[3] initially solved the structure of this phase through refinement of the neutron powder pattern in the orthorhombic space group *Imma*. The Li was located in five-coordinate interstitial sites (2× Li−O1 1.9658 Å; 2× Li−O2 2.0389 Å; Li−O1 2.1726 Å). In contrast, a recent theoretical study located the Li in four-coordinate sites.[4]

Recently, we addressed the chemical intercalation of lithium ions into anatase using *n*-butyllithium through XRD, $^6$Li and $^7$Li solid-state NMR, and X-ray absorption spectroscopy.[5] The solid-state MAS NMR spectra of the Li-intercalated samples are reproduced in Figure 1. In $Li_xTiO_2$ samples with $x \leqslant 0.3$ only one Li species with $\delta = 0$ ppm was observed by NMR while for $x > 0.3$ an additional, more abundant species with $\delta \sim 4$ ppm was observed. It was hypothesized that this second species is due to a weak Knight shift arising from the interaction of some Li ion sites with electrons in the anatase conduction band. Electronic correlation within the $t_{2g}$ and $e_g$ conduction band states, which become increasingly filled as $x$ increases, was evinced through the X-ray absorption pre-edge structure (XANES), which reflects the unoccupied density of states. The observation of two Li species by NMR spectroscopy suggests that previous refinements of neutron powder data, which located all of the lithium ions in five-coordinate interstitial sites, may be in doubt. To explain this discrepancy, it was hypothesized that Li ions occupying distinct crystallographic sites observable by NMR could not be distinguished on the basis of refinement of the neutron powder pattern due to disorder. In any event, it is considered that a revisitation of the neutron diffraction pattern of the stoichiometric phase is warranted.

In this study we examine in greater detail the effects of increasing Li intercalation on the crystallographic structure of anatase through Rietveld refinement of neutron powder data. At the same time changes in the magnetic and electronic structure are monitored through magnetic susceptibility measurements and electron paramagnetic resonance (EPR) spectroscopy.

## Experimental Section

The microcrystalline anatase used in this work was from Aldrich Chemical Co. and XRD showed it to be pure anatase. Previous studies[6] have shown by SEM that the particle size

* To whom correspondence should be addressed. Present address: Materials Division, Australian Nuclear Science and Technology Organization, PMB 1, Menai, NSW 2234, Australia. Tel.: 61-2-9717 3087. Fax: 61-2-9543 7179. E-mail: vlu@ansto.gov.au.

† University of New South Wales.

‡ Physics Division, Australian Nuclear Science and Technology Organization.

§ Monash University.

(1) Owen, J. R. *Chem. Soc. Rev.* **1997**, *26*, 256.

(2) Ceder, G.; Aydinol, M. K. *Solid State Ionics* **1998**, *109*, 151.

(3) Cava, R. J.; Murphy, D. W.; Zahurak, S.; Santoro, A.; Roth, R. S. *J. Solid State Chem.* **1984**, *53*, 64.

(4) Stashans, A.; Lunell, S.; Bergström, R. *Phys. Rev. B* **1996**, *53*, 159.

(5) Luca, V.; Hanley, T. L.; Roberts, N. K.; Howe, R. F. *Chem. Mater.* **1999**, *11*, 2089.

(6) Cabrera, M. I.; Alfano, O. M.; Cassano, A. E. *J. Phys. Chem.* **1996**, *100*, 20043.

10.1021/cm000504w CCC: $20.00 
Published on Web 03/02/2001

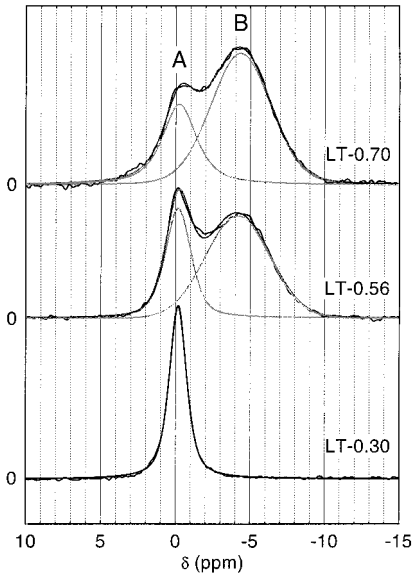


**Figure 1.** Room-temperature solid-state $^6$Li MAS NMR spectra of Li-intercalated anatase samples reproduced from Luca et al.[3]

range of this commercial anatase material ranges from 1000 to 2000 Å and light scattering has shown that when dispersed in water aggregates with an average diameter of about 3000 Å are present. Our own TEM, XRD, and light scattering measurements confirm these size ranges. Prior to treatment with *n*-butyllithium, the bulk microcrystalline anatase powders were conditioned by calcination in air at 400 °C for 24 h. Three 6.0-g samples of the conditioned microcrystalline anatase were transferred to Quickfit Pyrex vials where they were outgassed for about 1 h at 100 °C. To three separate samples of anatase were added 51.6, 25.8, and 12.9 mL, respectively, of the 1.44 M *n*-butyllithium/hexane solution. This was transferred to the sample vials under oxygen-free, dry argon gas on a Schlenk line and allowed to react for a prescribed interval of time at 60 °C. The amount of free hydroxide in the *n*-butyllithium solution was typically <0.3 M. All subsequent manipulations were carried out under an argon atmosphere. Usually, the sample changed color instantaneously and heat evolved. After the solution was left standing for 3 days, with occasional stirring, the anatase solid was allowed to settle, the supernatant removed under an argon atmosphere, and the solution analyzed for free *n*-butyllithium and hydroxide. Finally, the samples were washed with three portions of dry deoxygenated diethyl ether, then evacuated, with warming to 100 °C, and the vials sealed. From the amount of *n*-butyllithium remaining in the supernatants, it was deduced that the Li/Ti ratios of the three samples were 0.62, 0.49, and 0.24 ± 0.05. Titration of the hydroxide showed that all the free LiOH was recovered. All subsequent manipulations of the samples were performed in a nitrogen-filled glovebox. The solid samples, which had been exposed to ambient air, were analyzed by atomic absorption spectroscopy and found to possess Li/Ti ratios of 0.70, 0.56, and 0.30 ± 0.05 in agreement with the titration results. The samples will be referred to as LT-*x* where *x* is the Li/Ti ratio.

Variable temperature EPR data were recorded on either a Bruker ESP300 or a Bruker EMX spectrometer using a flow-through helium cryostat (Oxford Instruments). EPR simulations were carried out using the program SIMER.[7]

Neutron powder data were collected using the high-resolution powder diffractometer (HRPD) at the HIFAR reactor at the Australian Nuclear Science and Technology Organisation. The samples were packed into vanadium cans under a helium atmosphere and sealed using indium gaskets. The cans were rotated during measurement to avoid any preferred orientation. Patterns were recorded using 1.883 Å neutrons over a range $0 < 2\theta < 154°$ in 0.05° steps. Rietveld anlaysis was carried out using the program Rietica.[8]

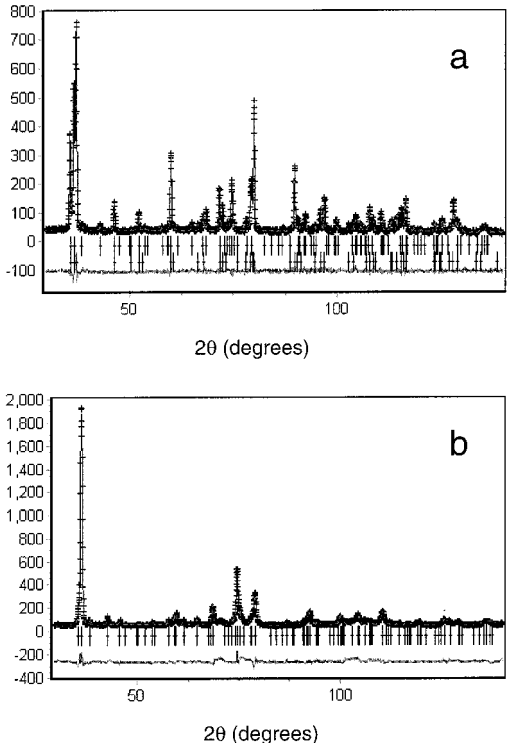


**Figure 2.** Refined room-temperature neutron diffraction pattern of (a) LT-0.30 and (b) LT-0.70.

Magnetic susceptibility measurements were performed on a Quantum Design MPM5 SQUID magnetometer operating in an applied field of 1 T. Samples of mass about 20 mg were contained in calibrated gelatine capsules, which were held firmly in the center of a drinking straw that was fixed to the sample rod. The instrument was calibrated using the accurately known magnetization of a palladium sample (Quantum Design) and against chemical calibrants such as $CuSO_4 \cdot 5H_2O$ and $[Ni(en)_3]S_2O_3$. The uncertainty in $\chi_m$ was $\pm 2 \times 10^{-6}$ cm$^3$ mol$^{-1}$.

## Results

As was previously observed,[3] refinement of the LT-0.56 composition proceeded smoothly in the space group *Imma*. This was also found to be the case for LT-0.30 and LT-0.70. Attempts to refine the structure in the space group *Imm*2 resulted in slightly inferior goodness-of-fit statistics, confirming the results of Cava et al.[3] The refined neutron diffraction pattern of the LT-0.30 sample is shown in Figure 2 and the structural parameters are given in Tables 1 and 2. Our previously reported X-ray diffraction data of LT-0.30 showed the existence of two phases comprising the unintercalated tetragonal anatase (*I* 4$_1$/*amd* No. 141) and the Li-intercalated orthorhombic phase (*Imma*). This was also apparent in the neutron diffraction pattern of LT-0.30 and therefore the refinement was carried out using a similar structural model comprising an orthorhombic lithium titanate phase and anatase. The Li occupancy

(7) Luca, V.; MacLachan, D. J. SIMER—a program for the nonlinear least squares fitting of EPR spectra using second-order perturbation theory, 1996.

(8) Hunter, B. A. Rietica—A Visual Rietveld Program. In *Commission on Powder Diffraction Newsletter*, Vol. 20, p 21, 1998. Available at http://www.iucr.org/iucr-top/comm/cpd/Newsletters/.

**Table 1. Unit Cell Parameters for $Li_xTiO_2$ Samples Derived by Refinement of Neutron Powder Data in Space Group *Imma***

| sample | *a* (Å) | *b* (Å) | *c* (Å) | particle diameter (Å) |
|---|---|---|---|---|
| $Li_{0.30}TiO_2$ | 3.801 | 4.075 | 9.054 | 732 |
| anatase core | 3.789 | 3.789 | 9.485 | 924 |
| $Li_{0.56}TiO_2$ | 3.809 | 4.075 | 9.046 | 473 |
| $Li_{0.70}TiO_2$ | 3.814 | 4.066 | 9.004 | 683 |
| bulk anatase[a] | 3.785 | 3.785 | 9.513 | 1274 |

[a] From refinement of laboratory X-ray data.

was refined in addition to the unit cell *z*-coordinate. The Li occupancy in the orthorhombic phase of LT-0.30, which constitutes about 66 mol % of the sample, was found to be 0.73, indicating that the intercalation does not occur uniformly throughout each crystallite but is rather restricted to a shell around a core of unintercalated anatase. Refinement of the anatase component in this sample gave similar *a* and *b* unit cell parameters to those obtained from the X-ray refinement of the precursor anatase and published data[9] but with a significantly reduced *c*-dimension. Intercalation also resulted in a decrease in the apparent anatase crystallite size. For the Li-intercalated orthorhombic component the unit cell parameters are close to the previously reported values[3] ($a = 3.8082$, $b = 4.0768$, $c = 9.0526$ Å) for refinement of an $Li_{0.50}TiO_2$ composition.

Although the neutron powder diffraction pattern of the LT-0.56 sample produced in this study also proceeded smoothly in space group *Imma*, our value for the *c*-dimension is somewhat smaller than that reported by Cava et al.[3] for a compound with stoichiometry of $Li_{0.5}TiO_2$. We also obtain a slightly different value of the Ti *z*-coordinate compared with that obtained by Cava et al. The Li occupancy factor refined to 0.71, which is close to that of the LT-0.30 phase. Further increase in the level of intercalation to $x = 0.70$ (Figure 2) gave a corresponding reduction in the *c*-dimension and a slight shift in the *z*-coordinate for both Li and Ti relative to that of the other samples. The Li occupancy factor for this sample was found to be slightly larger than that of the other two samples and again this was larger than the bulk stoichiometry.

Attempts were made to refine the neutron powder patterns in the *Imm*2 space group but these were consistently unstable, indicating that they were most likely over-determined. Refinment of pattern of the LT-0.56 phase recorded at 10 K data gave a Li thermal parameter that was larger than that obtained from the data measured at 298 K. Therefore, as far as neutron diffraction is concerned, the appropriate space group is *Imma* and on average a single Li environment is present.

The molar magnetic susceptibility, $\chi_m$, was measured over the temperature range 4−300 K for samples with the same bulk stoichiometry as those investigated by neutron diffraction. The molar susceptibilities show a weak temperature dependence from 50 to 300 K and then below 50 K a pronounced curvature is observed in the plot of $\chi_m$ versus *T* (Figure 3). The data for the three samples can be modeled well using the method of Johnston[10] and Harrison et al.[11] in their respective

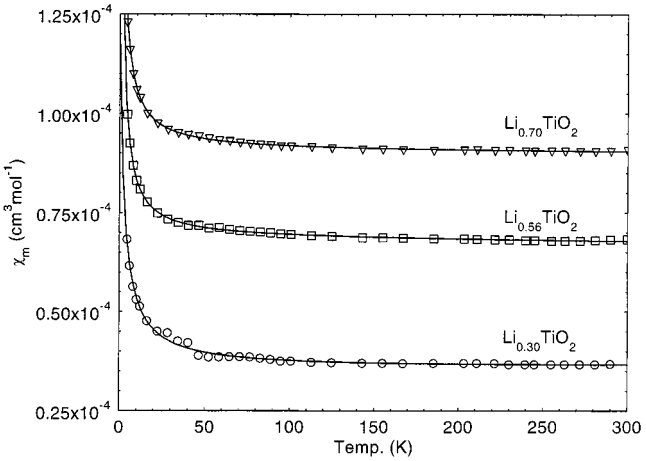


**Figure 3.** Magnetic susceptibility as a function of temperature and measured in an applied field of 1 T for different levels of intercalation. Solid lines through the data are the best fits using the expression $\chi = C_m/(T + \theta) + f(T)$.

**Table 2. Fractional Atomic Coordinates and Site Occupancies for $Li_xTiO_2$ Samples**

| | | fractional coordinates (Å) | | | | | | | |
|---|---|---|---|---|---|---|---|---|---|
| sample | atom | *x* | *y* | *z* | *N* | *B* | $R_p$ | $R_w$ | $\chi^2$ |
| $Li_{0.30}TiO_2$ | Ti | 0.0000 | 0.2500 | 0.8849 | 1 | 1.05 | 6.56 | 8.23 | 2.31 |
| | O1 | 0.0000 | 0.2500 | 0.1030 | 1 | 0.92 | | | |
| | O2 | 0.0000 | 0.2500 | 0.6510 | 1 | 0.63 | | | |
| | Li | 0.0000 | 0.2500 | 0.3398 | 0.70 | 0.89 | | | |
| anatase | Ti | 0.0000 | 0.2500 | −0.1250 | | | | | |
| | O | 0.0000 | 0.2500 | 0.08379 | | | | | |
| $Li_{0.56}TiO_2$ | Ti | 0.0000 | 0.2500 | 0.8792 | 1 | 1.20 | 7.49 | 9.17 | 4.44 |
| | O1 | 0.0000 | 0.2500 | 0.1018 | 1 | 0.75 | | | |
| | O2 | 0.0000 | 0.2500 | 0.6516 | 1 | 1.20 | | | |
| | Li | 0.0000 | 0.2500 | 0.3424 | 0.72 | 0.83 | | | |
| $Li_{0.70}TiO_2$ | Ti | 0.0000 | 0.2500 | 0.8828 | 1 | 1.67 | 9.40 | 12.02 | 7.15 |
| | O1 | 0.0000 | 0.2500 | 0.1026 | 1 | 0.95 | | | |
| | O2 | 0.0000 | 0.2500 | 0.6502 | 1 | 1.17 | | | |
| | Li | 0.0000 | 0.2500 | 0.3365 | 0.79 | 1.27 | | | |

**Table 3. Magnetic Parameters Determined from Fitting of the Susceptibility Data in Figure 3**

| sample | Curie constant, $C_m$ ($10^{-4}$ cm$^3$ mol$^{-1}$) | Weiss constant, $\theta$ (K) | $B_m$ ($10^{-9}$) | $A_m$ ($10^{-5}$) |
|---|---|---|---|---|
| $Li_{0.30}TiO_2$ | 2.39 | 2.72 | 2.32 | 3.52 |
| $Li_{0.56}TiO_2$ | 1.56 | 0.44 | −3.45 | 6.84 |
| $Li_{0.70}TiO_2$ | 1.71 | 0.71 | −1.56 | 9.03 |

investigations of the $Li_{1+x}Ti_{2-x}O_4$ spinel system. In this analysis the data can be fit to a function with two terms, a Curie−Weiss term, $C_m/(T + \theta)$ due to localized electrons, and a weakly temperature-dependent term, $f(T)$, from conduction electrons:

$$\chi = C_m/(T + \theta) + f(T)$$

$f(T)$ is a linear function, $f(T) = A_m + B_mT$. The $B_m$ parameter undergoes a transition from a positive value for $x = 0.30$ to a negative value for $x \geq 0.5$. In the spinel system this transition from positive to negative slope occurs as *x* decreases and the samples become conducting; that is, an insulator-to-metal transition is traversed. The Curie constants for the present samples (Table 3) are about an order of magnitude less than those observed in the spinel system. From this susceptibility

(9) Howard, C. J.; Sabine, T. M.; Dickson, F. *Acta Crystallogr.* **1991**, *B47*, 462.

(10) Johnston, D. C. *J. Low Temp. Phys.* **1976**, *25*, 145−175.

(11) Harrison, M. R.; Edwards, P. P.; Goodenough, J. B. *J. Solid State Chem.* **1984**, *54*, 136.

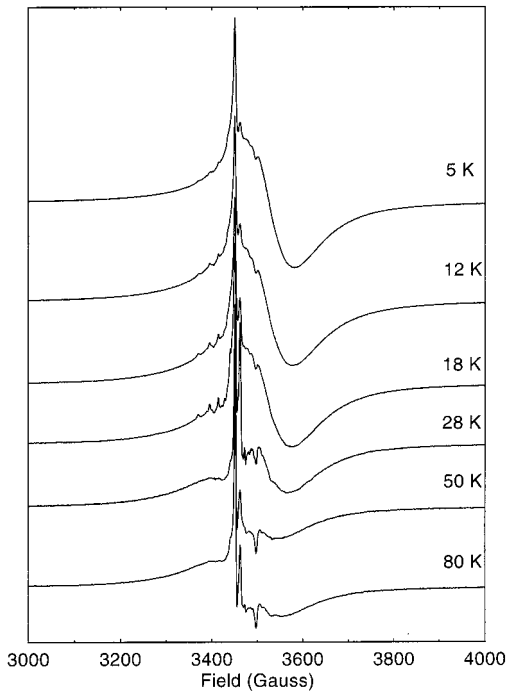


**Figure 4.** 9.533 GHz EPR spectra of LT-0.30 as a function of temperature.

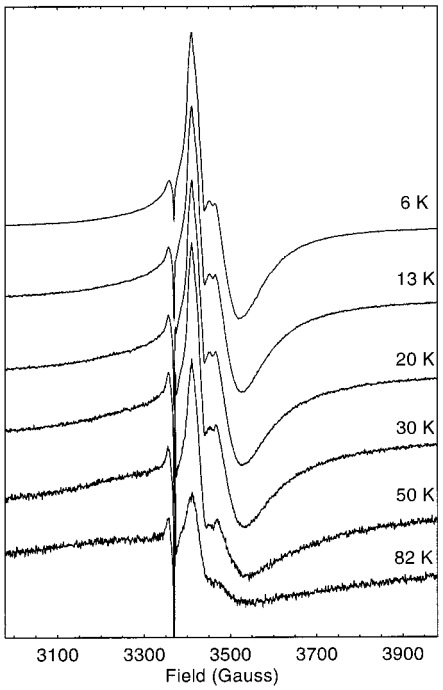


**Figure 5.** 9.453 GHz EPR spectra of LT-0.70 as a function of temperature.

**Table 4. EPR Simulation Parameters for Selected Li-intercalated Anatase Samples**

| sample | $g_{xx}$ | $g_{yy}$ | $g_{zz}$ | $\Gamma_{xx}$ (G) | $\Gamma_{yy}$ (G) | $\Gamma_{zz}$ (G) |
|---|---|---|---|---|---|---|
| $Li_{0.30}TiO_2$ | 1.973 | 1.924 | 1.893 | 11.0 | 109.0 | 176.1 |
| | 1.939 | 1.939 | 1.939 | 339.1 | 339.1 | 339.1 |
| $Li_{0.56}TiO_2$ | 1.971 | 1.924 | 1.893 | 37.3 | 98.9 | 377.2 |
| $Li_{0.70}TiO_2$ (oxidized)[a] | 2.0036 | 2.0036 | 2.0050 | 0.5 | 0.5 | 0.3 |

[a] Oxidized by prolonged exposure to ambient air.

data assuming $g = 2.0$, we calculate that the percentage of d electrons localized on Ti to give $Ti^{3+}$ is between 2 and 4% at 4 K for the three samples.

To investigate the nature of localized electronic moments in the various Li-intercalated anatase samples, EPR spectra were recorded at a range of temperatures from 4 to 100 K. EPR spectra of the LT-0.30 sample are shown in Figure 4. A sharp intense signal and a broad signal predominate in these spectra and they persist up to about 100 K. Superimposed on the broad signal are a group of narrow lines that are centered at about 3450 G. The contributions that the different resonances make to the total spectrum varies with increasing temperature but there is little change in line width. The 18 K spectrum could be simulated well (Figure 6a) in terms of two paramagnetic species. Species A corresponds to the narrow signal, which has an orthorhombic **g** tensor ($g_{xx} = 1.973$, $g_{yy} = 1.924$, and $g_{zz} = 1.893$; $g_{ave} = 1.93$) with anisotropic line width (Table 4). The average $g$ value is close to that of interstitial $Ti^{3+}$ ions ($d^1$) in oxygen-deficient rutile, which have $g_{||} = 1.941$ and $g_{\perp} = 1.976$ ($g_{ave} = 1.964$)[12,13] The Hamiltonian parameters are also similar to those observed for $Ti^{3+}$ in the framework of zinc titanosilicate ($g = 1.979$; $g = 1.900$)[14] and in the Ti-containing zeolite TS-1.[15] When the spectra are converted to the second derivative, it is evident that the weak structure that is superimposed on the broad resonance near 3450 G consists of at least an eight-line spectrum with a 24 G splitting. The structure is therefore presumed to be $^{47}Ti$ or $^{49}Ti$ ($I = 7/2$) hyperfine or superhyperfine.

The broad resonance (species B) centered at $g = 1.939$ is the average of the three **g**-tensor components for species A. We chose to ignore the weak multiline in the simulations because the lines are not adequately resolved.

The EPR spectra of LT-0.70 recorded at various temperatures are given in Figure 5. Although the spectra show a pronounced broadening compared to the spectra of LT-0.30 where the Li content is much lower, a satisfactory simulation could be carried out (Figure 6b) in terms of a single species with very similar **g**-tensor parameters except that, as expected, all the line width components are much larger. In the spectra of Figure 5, a very sharp feature is observed at $H = 3375$ G. To understand this feature, samples were exposed to air for extended periods of time to effect the reoxidation and removal of the $Ti^{3+}$ EPR. For a sample with composition $Li_{0.63}TiO_2$, this aerial oxidation gave the spectrum shown in Figure 6c, which could be simulated using the parameters shown in Table 4. These parameters are most compatible with those of $O_3^{3-}$ ($g_{||} = 2.008$ and $g_{\perp} = 2.001$)[16] rather than the superoxide ions ($O_2^-$) adsorbed on titania surfaces[17] or $O^-$, which usually has $g_{||} < g_{\perp}$.[18] The formation of $O_3^{3-}$ may occur by the

(12) Aono, M.; Hasiguti, R. R. *Phys. Rev. B: Condens. Matter* **1993**, *48*, 12406.
(13) Hasiguti, R. R. *Ann. Rev. Mater. Sci.* **1972**, *2*, 69.
(14) Luca, V.; MacLachlan, D. J.; Howe, R. F.; Bramley, R. *J. Mater. Chem.* **1995**, *5*, 557.
(15) Tuel, A.; Diab, J.; Gelin, P.; Dufaux, M.;. Dutel J.-F.; Ben Taarit, Y. *J. Mol. Catal.* **1990**, *63*, 95.
(16) Meriaudeau, P.; Vedrine, J. C. *J. Chem. Soc., Faraday 1* **1976**, *72*, 472.
(17) Anpo, M.; Che, M.; Fubini, B.; Garrone, E.; Giamello, E.; Paganini, M. C. *Top. Catal.* **1999**, *8*, 189−199.
(18) Che, M.; Tench, A. J. *Adv. Catal.* **1982**, *31*, 77.

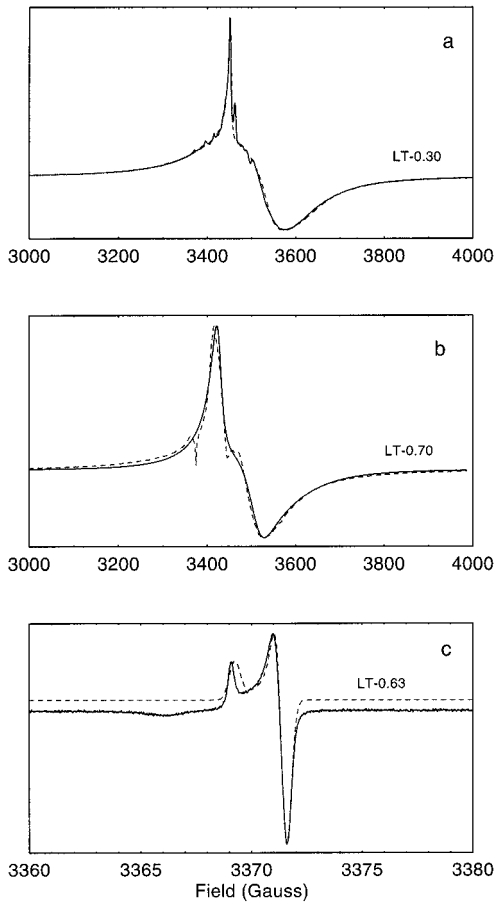


**Figure 6.** Simulated EPR spectra of (a) LT-0.30 recorded at 18 K, (b) LT-0.70 recorded at 4 K, and (c) LT-0.63 after prolonged exposure to ambient air and recorded at 80 K.

reaction of molecular oxygen with a lattice oxide ion according to $Ti{-}O^{2-} + O_2 \rightarrow O_3^{3-}$ as postulated by Meriaudeau and Vedrine.[16]

When the reciprocal integrated intensity of the EPR spectra obtained for both samples are plotted as a function of temperature, a linear relationship is obtained up to at least 70 K (Figure 7). There is some deviation at higher temperatures for the LT-0.56, but as the spectra have very little intensity by this stage, the uncertainty of the integrated value is high. For LT-0.70 the departure from Curie−Weiss behavior appears to be more significant, suggesting that at these higher Li contents there may be some interaction between $Ti^{3+}$ spins. Since the temperature dependence of the spectra obeys the Curie−Weiss law, this confirms that the electronic moments are due to localized and isolated $Ti^{3+}$. The concentrations of the localized moments observed by EPR were measured and values of 0.004, 0.003, and 0.003 spins per Ti were obtained for LT-0.30, LT-0.56, and LT-0.70, respectively. This indicates that the number of localized moments represents only a small fraction of the number of intercalated Li cations and hence of the total number of electrons introduced into the system. EPR, however, can only detect those moments with relaxation times that are longer than the EPR time scale. Also, the fact that the spin concentrations are similar, regardless of the amount of Li intercalated, implicates a surface reaction that goes to completion, even for $x < 0.3$.

## Discussion

Since the particle size distribution of the present commercial anatase samples is quite narrow, and as-

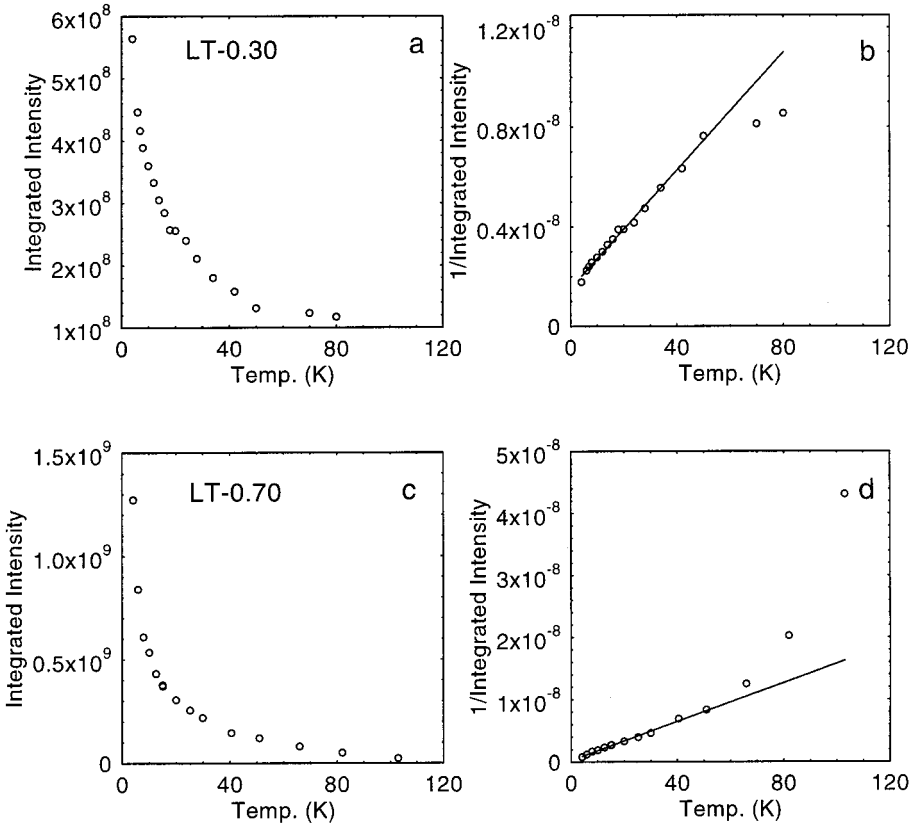


**Figure 7.** Temperature dependence of the second-derivative (left) and reciprocal second-derivative (right) EPR intensity for LT-0.30 (a and b) and LT-0.70 (c and d).

suming that the intercalation reaction front proceeds at a constant rate for each particle, then it is expected that most of the particles in samples reacted with lithium concentrations well below the stoichiometric value (i.e., LT-0.3) should consist of a shell of the orthorhombic phase and an anatase core.

Neutron refinement of the LT-0.30 sample confirms that these partially intercalated anatase particles have a core−shell structure consisting of an orthorhombic $Li_xTiO_2$ shell that is about 720-Å thick, while the core, with a diameter of 920 Å, has the anatase structure. The $Li_xTiO_2$ shell phase can be refined well in the orthorhombic space group *Imma* with the Li occupancy close to that of the fully intercalated LT-0.70 phase. However, the lattice parameters of the anatase core (Table 1) seem to be significantly altered compared to bulk anatase. This suggests that a significant distortion of the anatase lattice precedes the intercalation step. As $x$ increases beyond 0.3, the domain size of the orthorhombic phase increases without any significant change in the Li occupancy. There appears to be a real increase in the *a*-dimension and a decrease in the *c*-dimension of the unit cell as Li is progressively intercalated. Attempts to refine these neutron powder patterns on an *Imm*2 unit cell resulted in a worsening of the goodness-of-fit parameters, indicating that *Imma* is the more appropriate space group. Although the Li thermal parameters do not change appreciably on going from $x = 0.3$ to $x = 0.56$, the thermal parameter of O2 increases 2-fold (Table 2). There is also an increase in the thermal parameter for Ti but this is not as severe.

Although NMR data clearly show the presence of two Li sites, repeated attempts to refine the structure in the space group *Imm*2, with two independent Li sites, were consistently unstable and hence were most likely overdetermined. Neutron powder diffraction data were also recorded at 10 K for the $Li_{0.5}TiO_2$ phase. The refinement in *Imma* produced larger thermal parameters at low temperature for the Li site, while refinement in *Imm*2 gave negative thermal parameters at low temperature. We believe that these data highlight the fact that static disorder dominates over thermal disorder for the Li sites. In effect, there is no long-range order of Li ions on the two sites detected by NMR, so that as far as neutron diffraction is concerned, there is only one site.

The susceptibility of LT-0.30 shows no evidence of conducting domains and the $^6$Li NMR spectrum shows only a single Li species whose chemical shift is consistent with five-coordinate Li as indicated by the neutron diffraction data. Therefore, the $^6$Li NMR spectrum consisting of a single resonance at $\delta = 0$ ppm[5] can be assigned to Li in five-coordinate interstitial sites of the orthorhombic phase. It has been shown that as $x$ increases from 0.3 to 0.56, a second shifted Li species is observed by NMR that has about the same intensity (Figure 1). The neutron refinement of LT-0.56 shows no dramatic change in the parameters of the orthorhombic phase with respect to LT-0.3. This begs the question of the origin of the second Li species observed by NMR.

It was previously hypothesized[5] that the second NMR species (species B) originates from Li in slightly different structural sites to species A and that in these sites a direct interaction occurs between Li and conduction band electrons. The present magnetic susceptibility measurements indicate that the samples become conducting as the level of intercalation increases beyond $x = 0.30$. EPR indicates that few of the injected electrons become localized on Ti atoms. This supports the previous interpretation of the species B resonance observed in the NMR spectrum of samples with $x > 0.3$.[5]

To conclude, although refinement of the neutron powder pattern in the *Imma* space group with a single type of Li environment is preferred to *Imm*2 on goodness-of-fit grounds, the presence of two distinct Li environments in the present titanate compounds cannot be disputed. The inability for these two environments to be expressed in the neutron refinements is a result of static disorder, which blurs this distinction.

CM000504W